Molecular Biology of the Cell
Vol. 13, 169–182, January 2002

Dynamin-dependent Transferrin Receptor Recycling by Endosome-derived Clathrin-coated Vesicles

Ellen M. van Dam and Willem Stoorvogel*

Department of Cell Biology, University Medical Center and Institute of Biomembranes, Utrecht University, 3584 CX Utrecht, The Netherlands

Submitted July 31, 2001; Revised September 20, 2001; Accepted October 2, 2001
Monitoring Editor: Juan Bonifacino

Previously we described clathrin-coated buds on tubular early endosomes that are distinct from those at the plasma membrane and the trans-Golgi network. Here we show that these clathrin-coated buds, like plasma membrane clathrin-coated pits, contain endogenous dynamin-2. To study the itinerary that is served by endosome-derived clathrin-coated vesicles, we used cells that overexpressed a temperature-sensitive mutant of dynamin-1 (dynamin-1^{G273D}) or, as a control, dynamin-1 wild type. In dynamin-1^{G273D}–expressing cells, 29–36% of endocytosed transferrin failed to recycle at the nonpermissive temperature and remained associated with tubular recycling endosomes. Sorting of endocytosed transferrin from fluid-phase endocytosed markers in early endosome antigen 1-labeled sorting endosomes was not inhibited. Dynamin-1^{G273D} associated with accumulated clathrin-coated buds on extended tubular recycling endosomes. Brefeldin A interfered with the assembly of clathrin coats on endosomes and reduced the extent of transferrin recycling in control cells but did not further affect recycling by dynamin-1^{G273D}–expressing cells. Together, these data indicate that the pathway from recycling endosomes to the plasma membrane is mediated, at least in part, by endosome-derived clathrin-coated vesicles in a dynamin-dependent manner.

INTRODUCTION

Plasma membrane proteins can be removed selectively and efficiently from the cell surface through endocytic uptake by clathrin-coated vesicles. Proteins carried by plasma membrane-derived clathrin-coated vesicles are first delivered to sorting endosomes. From there they are targeted to lysosomes, the trans-Golgi network (TGN), or the recycling compartment. At the recycling compartment membrane, proteins can be distributed further to the TGN or, in polarized cells, to the opposing plasma membrane domain. Most membrane proteins in the recycling compartment are, however, efficiently transported back to the plasma membrane (reviewed by Mellman, 1996). Recycling membrane proteins are thought to exit from vacuolar sorting endosomes via attached tubular extensions (Hopkins and Trowbridge, 1983; Geuze *et al.*, 1987; Mayor *et al.*, 1993; Hopkins *et al.*, 1994). The recycling compartment is, in contrast to tubulovesicular sorting endosomes, composed of tubular membranes only and concentrated predominantly in the perinuclear area. Vesicular transport intermediates between sorting endosomes, recycling endosomes, and the plasma membrane have not been identified, and the mechanism for transport between these compartments has not been resolved.

The transferrin (Tf) receptor (TfR) and its ligand Tf have been used extensively as markers of the recycling pathway. Endocytosed TfR/Tf complexes recycle to the plasma membrane with the same kinetics as certain lipids (Mayor *et al.*, 1993) and independently of the TfR cytoplasmic domain (Johnson *et al.*, 1993). These data indicate that TfR recycling, in contrast to uptake, can occur without active recruitment in recycling vesicles by cytosolic coat proteins. In polarized cells, however, endocytosed TfR is efficiently sorted from the transcytotic pathway and recycled to the basolateral plasma membrane (Mellman, 1996; Odorizzi and Trowbridge, 1997; Futter *et al.*, 1998), indicating that recruitment mechanisms do exist. Only a few molecular players have been identified so far to function in the TfR recycling pathway. At least two Rab proteins have been implicated, Rab4 (van der Sluijs *et al.*, 1992; Sheff *et al.*, 1999) and Rab11 (Ullrich *et al.*, 1996; Ren

Article published online ahead of print. Mol. Biol. Cell 10.1091/mbc.01–07-0380. Article and publication date are are at www.molbiolcell.org/cgi/doi/10.1091/mbc.01–07-0380.

* Corresponding author. E-mail address: w.stoorvogel@lab.azu.nl.

Abbreviations used: BFA, brefeldin A; BSA, bovine serum albumin; DAB, diaminobenzidine tetrahydrochloride; dyn^{ts}, dynamin-1^{G273D}; dyn^{wt}, wild type dynamin-1; EEA1, early endosome antigen 1; F-dextran, fluorescein-conjugated dextran; HA, hemagglutinin; ^{125}I-Tf-SS-biotin, biotinylated ^{125}I-Tf; Ig, immunoglobulin; MES, 2-(*N*-morpholino) ethanesulfonic acid; MESNA, 2-mercaptoethanesulfonic acid; PBS, phosphate-buffered saline; TaR-Tf, Texas Red-conjugated transferrin; Tf, transferrin; TfR, transferrin receptor; Tf/HRP, horseradish peroxidase-conjugated transferrin; TGN, trans-Golgi network.

et al., 1998; Wilcke *et al.*, 2000). Dominant-negative mutants of these GTPases have, however, limited and distinct effects on the routing and kinetics of TfR recycling. Similarly, interference with the function of the soluble *N*-ethylmaleimide-sensitive fusion proteins syntaxin 13 (Prekeris *et al.*, 1998) or cellubrevin (Galli *et al.*, 1994) only partially affected TfR recycling, as did interference with class I phosphatidylinositol 3-kinase (Siddhanta *et al.*, 1998) or RME-1 (Lin *et al.*, 2001) function. None of the above players seem to be responsible for recycling of the full complement of endocytosed TfR, suggesting that parallel recycling pathways and/or molecular mechanisms are involved. Previously, we reported clathrin-coated buds on early endosomal tubules and distinguished these from plasma membrane-derived clathrin-coated vesicles by size, continuity with endosomes, and lack of the adaptor protein complex AP-2 (Stoorvogel *et al.*, 1996). These buds contained TfR, suggesting that endosome-derived clathrin-coated vesicles may function in the recycling pathway. TfR-containing clathrin-coated buds have also been observed on endosomes in polarized Madin-Darby canine kidney cells in which they were proposed to play a role in basolateral TfR trafficking (Futter *et al.*, 1998).

Dynamins are thought to assist the formation of transport vesicles from diverse donor compartments (reviewed by Urrutia *et al.*, 1997; Marsh and McMahon, 1999; van der Bliek, 1999), including clathrin-coated vesicles from the plasma membrane (Herskovits *et al.*, 1993; van der Bliek *et al.*, 1993; Damke *et al.*, 1994, 1995a). Dominant-negative mutants of the ubiquitously expressed dynamin-2 and the neuronal dynamin-1 interfered with pinching of clathrin-coated vesicles from the plasma membrane (Damke *et al.*, 1994, 1995a; Altschuler *et al.*, 1998). Although TfR uptake was severely affected by dynamin-1^{K44A} and dynamin-2^{K44A} mutants, TfR recycling proceeded normally, and it was thus concluded that dynamin does not play an essential role in TfR recycling (Altschuler *et al.*, 1998). Dynamin-1^{G273D} (dyn^{ts}), a dynamin-1 mutant corresponding to the *Drosophila shibire*^{ts1} allele, also had a dramatic effect on TfR uptake (Damke *et al.*, 1995a). To our knowledge, the effect of dyn^{ts} on TfR recycling has not been studied previously. Here we demonstrate that dyn^{ts} interfered with the recycling of endocytosed Tf and with the budding of clathrin-coated vesicles from endosomes. These observations, together with other evidence, indicate a role for dynamin in a clathrin-driven recycling pathway.

MATERIALS AND METHODS

Cell Culture and Analysis

Nontransfected tTA-HeLa cells (Gossen and Bujard, 1992) were cultured at 37°C in DMEM supplemented with 10% fetal calf serum, 100 U/ml streptomycin/penicillin, and 400 μg/ml G418. Stably transformed tTA-HeLa cells with a tightly regulated expression of hemagglutinin (HA)-tagged wild-type dynamin-1 (dyn^{wt}) or dynamin-1^{K44A} (Damke *et al.*, 1995b) or dyn^{ts} (Damke *et al.*, 1995a) were generously provided by Dr. S.L. Schmid (Scripps Research Institute, La Jolla, CA) and expanded at 37°C in DMEM supplemented with 10% fetal calf serum, 100 U/ml streptomycin/penicillin, 400 μg/ml G418, 200 ng/ml puromycin, and 2 μg/ml tetracycline. To induce dynamin-1 expression, cells were washed five times with phosphate-buffered saline (PBS), seeded in the absence of tetracycline, and cultured at 32°C during which the culture medium was refreshed every 24 h. To measure expression of HA-tagged dynamin-1, cells were lysed directly in SDS sample buffer containing β-mercaptoethanol and analyzed by Western blotting using monoclonal mouse anti-HA (12CA5 from BabCO, Richmond, CA). As a control, tubulin was detected with rabbit anti-tubulin, α-T13 (generously provided by Dr. T.E. Kreis [Kreis, 1987]). Antibodies were detected by chemiluminescence using standard procedures.

Transport Assays

Tf (Sigma, St. Louis, MO) was saturated with Fe^{3+} and labeled with ^{125}I using iodo-beads (Pierce Chemicals, Indianapolis, IN) according to standard procedures. When indicated, ^{125}I-Tf was biotinylated (^{125}I-Tf-SS-biotin) using sulfo-NHS-SS-biotin (Pierce).

For uptake assays, cells were first depleted from serum Tf by extensive washing, followed by a 30-min incubation in transport medium (MEM buffered with 20 mM HEPES/NaOH, pH 7.4, containing 0.1% bovine serum albumin [BSA]) in a water bath at 30°C. Tf-depleted cells were then preincubated in transport medium for 30 min at 25 or 38°C in the absence of ligand, after which ^{125}I-Tf (2 μg/ml) was endocytosed at the same temperature for the indicated time. Nonbound ligand was removed by extensive washing at 0°C. Plasma membrane-bound ^{125}I-Tf was removed at 0°C during subsequent 10-min incubations at pH 5.0 (20 mM 2-(*N*-morpholino)ethanesulfonic acid [MES] pH 5, 130 mM NaCl, 50 μM desferal, 2 mM $CaCl_2$, and 0.1% BSA) and pH 7.4 (transport medium containing 50 μM desferal). Internalized ^{125}I-Tf was collected by solubilizing the cells in 1 N NaOH and expressed as the percentage of total cell associated ^{125}I-Tf (intracellular plus plasma membrane). The data were corrected for nonspecific cell-associated ^{125}I-Tf (<10%) as determined in parallel experiments in which an excess (200 μg/ml) of nonlabeled Tf was present during loading.

For recycling assays, endosomes were first loaded with ^{125}I-Tf as indicated above for 1 h at 16, 25, or 38°C. Plasma membrane-bound ^{125}I-Tf was removed at 0°C by subsequent 10-min incubations at pH 5.0 (20 mM MES, pH 5, or 20 mM sodium actate/acetic acid pH 5, in 130 mM NaCl, 50 μM desferal, 2 mM $CaCl_2$, and 0.1% BSA) and pH 7.4 (transport medium containing 50 μM desferal). Cells were then incubated at 25 or 38°C in transport medium containing 50 μM desferal in the presence or absence of 10 μg/ml brefeldin A (BFA) (Sigma) or 100 nM concanamycin A (Sigma), and the release of ^{125}I-Tf was determined as described previously (van Weert *et al.*, 1995). The data were corrected for nonspecific ^{125}I-Tf (<10%) as determined in parallel experiments in which an excess (200 μg/ml) of nonlabeled Tf was present during loading. For experiments with ^{125}I-Tf-SS-biotin, cells were pulse-chased at 38°C as indicated above. After the chase, these cells were transferred to 0°C and incubated three times for 30 min at 0°C with 10 mM 2-mercaptoethanesulfonic acid (MESNA) in 100 mM NaCl, 50 mM Tris-HCl, pH 8.6, to cleave off the biotin moiety from plasma membrane-associated ^{125}I-Tf-SS-biotin. Excess MESNA was then quenched with 50 mM iodoacetamide in PBS. After the MESNA treatment, the cells were lysed in transport medium containing 1% Triton X-100, 1 μM leupeptin, 1 μM pepstatin, and 1 mM phenylmethylsulfonyl fluoride. Nuclei were removed from the lysates by centrifugation at 6000 rpm for 5 min in an Eppendorf centrifuge. ^{125}I-Tf-SS-biotin was collected with >90% efficiency from the lysates and the release media by adsorption to streptavidin beads (Sigma). The data were corrected for nonspecific ^{125}I-Tf-SS-biotin as determined in parallel experiments (see above). For all recycling assays, kinetic parameters were obtained by fitting data into a single exponential decay equation with three parameters, $y = y_0 + ae^{bt}$.

Confocal Laser Scanning Microscopy

dyn^{wt} and dyn^{ts} cells were cultured as above on glass coverslips in the absence of tetracycline. The cells were washed and preincubated for 30 min at 30°C in transport medium, followed by a 30- or 60-min incubation at 38°C in the presence or absence of 1 mg/ml lysine-fixable fluorescein-conjugated dextran, M_r 10,000 (F-dextran; Molec-

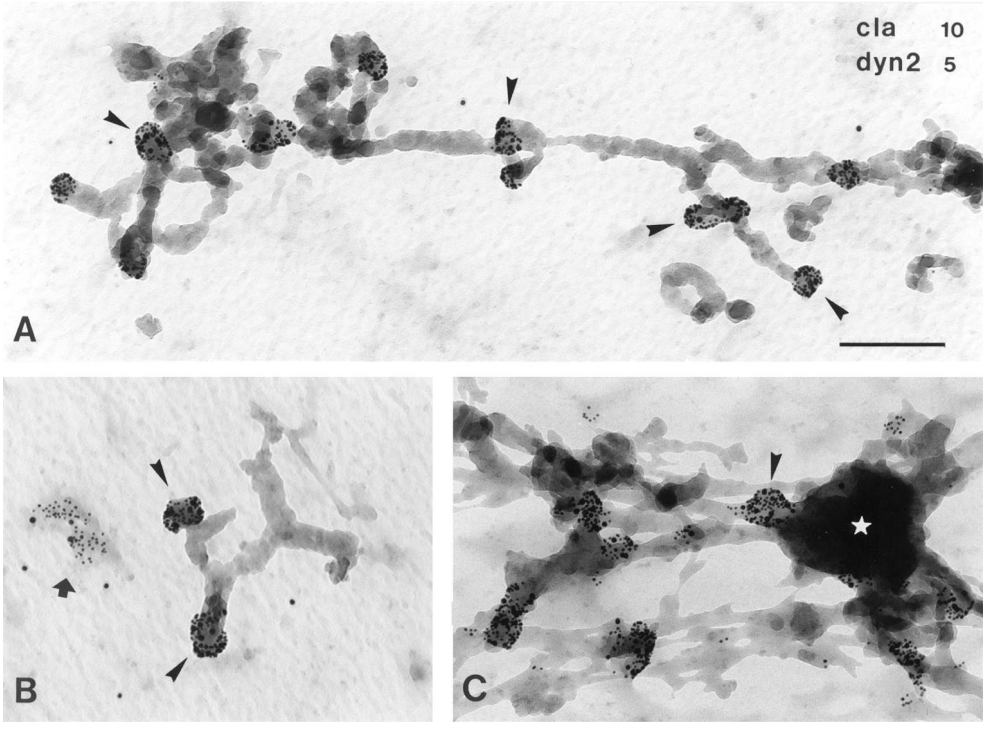

Figure 1. Clathrin-coated buds on endosomes contain endogenous dynamin. Nontransfected HeLa cells were incubated in the presence of Tf/HRP for 60 min at 37°C, and processed for whole mount immunoelectron microscopy. Samples were immuno-double–labeled for clathrin (cla, 10-nm gold) and endogenous dynamin-2 (dyn2, 5-nm gold) using polyclonal anti-clathrin and monoclonal HUDY-1, respectively. (A–C) Tubular early endosomes varied in length (compare A with B), but all were decorated with buds that labeled for both clathrin and dynamin-2 (for examples, see arrowheads). For quantification, see Figure 9A. (B) A large electron-lucent dynamin/clathrin-coated pit at the plasma membrane (arrow) is clearly different from DAB-contrasted 60-nm buds on endosomes (arrowheads). (C) Occasionally, tubules and buds (arrowhead) seem to associate with early endosomal vacuoles (asterisk). Bar, 200 nm.

ular Probes, Eugene, OR) and/or 20 μg/ml Texas Red-conjugated Tf (TaR-Tf) (Molecular Probes). After uptake, the cells were washed at 0°C, and plasma membrane-associated TaR-Tf was removed using the procedure described above for dissociation of plasma membrane-bound ^{125}I-Tf. Cells were then either fixed directly with 4% paraformaldehyde in 0.1 M phosphate buffer or chased for 60 min at 38°C and then fixed. Fixed cells were washed with PBS, and free aldehyde groups were quenched with 50 mM NH_4Cl in PBS. The cells were then either mounted directly or first processed for immunolabeling. For immunolabeling, the cells were permeabilized and labeled in PBS containing 0.1% saponin and 2% BSA, using standard procedures. Overexpressed dynamin-1 and endogenous TfR were labeled with polyclonal goat anti–dynamin-1 (Santa Cruz Biotechnology, Santa Cruz, CA) and the monoclonal mouse antibody HTR-H68.4 (White *et al.*, 1992; Zymed Laboratories, South San Francisco, CA), respectively. Polyclonal sheep anti-human TGN46 was from Serotec (Oxford, UK) and monoclonal mouse anti-early endosome antigen 1 (EEA1) was from Transduction Laboratories (Lexington, KY). Primary antibodies were detected with fluorescein isothiocyanate-conjugated donkey anti-goat immunoglobulin (Ig) G, Texas Red-conjugated donkey anti-mouse IgG, ALEXA-conjugated donkey anti-sheep IgG, or fluorescein isothiocyanate-conjugated goat anti-mouse IgG (all from Jackson Immunoresearch Laboratories, West Grove, PA). Coverslips were washed and embedded in Mowiol containing 2.5% 1,4-diazobicyclo-[2.2.2]-octane (Sigma), and optical sections were analyzed by confocal laser scanning microscopy using a TCS 4D system (Leica, Wetzlar, Germany). When indicated, serial 0.3-μm optical sections were superimposed to obtain an integrated view of entire cells.

Whole Mount Immunocytochemistry

Whole mount immunocytochemistry was performed as described by Stoorvogel *et al.* (1996) with minor modifications. Cells were cultured on golden grids carrying carbon-coated Formvar films that were first soaked in 1% gelatin for 1 h, washed, and fixed for 10 min with 0.5% glutaraldehyde in PBS. Horseradish peroxidase-conjugated Tf (Tf/HRP) was prepared as described by (Stoorvogel *et al.* (1988). Cells on grids were washed with transport medium and then incubated in the presence of 25 μg/ml Tf/HRP for either 1 h at 25°C followed by 5 min at 38°C (dyn^{wt} and dyn^{ts} cells) or 1 h at 37°C (nontransfected cells). Tf/HRP-containing endosomes were selectively fixed with diaminobenzidine tetrahydrochloride (DAB) (BDH, Poole, Dorset, UK), after which the cells were permeabilized with saponin and then fixed with 2% paraformaldehyde and 0.2% glutaraldehyde in 0.1 M phosphate buffer, pH 7.4. The cytoplasmic domain of the TfR was labeled with HTR-H68.4 (see above). Affinity-purified rabbit polyclonal anti-clathrin was kindly provided by Dr. Corvera (University of Massachusetts, Worcester, MA). Dynamin-1 and endogenous dynamin-2 were labeled with polyclonal anti–dynamin-1 (see above) and monoclonal HUDY-1 (Upstate Biotechnology, Lake Placid, NY), respectively. Monoclonal antibodies directed against clathrin heavy chain, X22, and α-adaptin, AP.6 (Chin *et al.*, 1989) were kindly provided by Dr. Brodsky (University of California, San Francisco, CA). Monoclonal mouse and polyclonal goat antibodies were detected with rabbit anti-mouse Ig and rabbit anti-goat (see above), respectively, followed by protein A-gold.

RESULTS

Endosome-associated Clathrin-coated Buds Contain Endogenous Dynamin

Previously, we characterized a novel class of clathrin-coated buds on endosomes with a technique that allows immunoelectron microscopic examination of endosomes in nonsectioned cells (Stoorvogel *et al.*, 1996). These buds contain TfR, suggesting that they might recycle endocytosed membrane proteins. Because dynamin-2 functions in pinching off clathrin-coated vesicles from the plasma membrane, we studied whether this endogenous dynamin also localizes to endo-

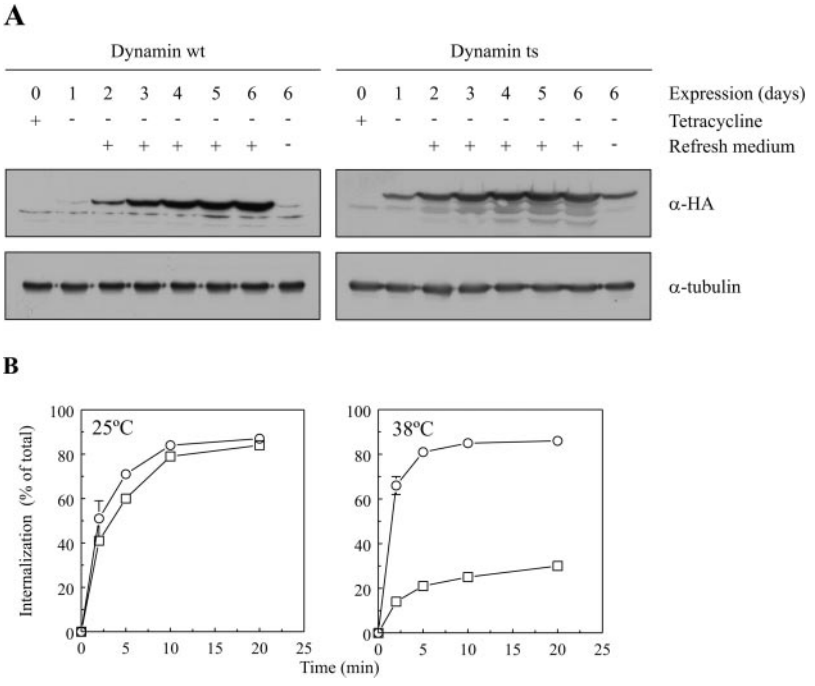

Figure 2. Expression of dyn^{wt} and dyn^{ts} and the effects on TfR internalization. (A) Cells were cultured for 6 d at 32°C in the presence (+) or absence (−) of tetracycline for the last 1–6 d. After extensive washing and replacement of tetracycline-containing medium by tetracycline-lacking medium, medium was either left on the cells for 6 d (− refresh medium) or refreshed daily (+ refresh medium). Western blots of cell lysates were probed with anti-HA antibodies to demonstrate HA-tagged dyn^{wt} or dyn^{ts} and with anti-tubulin antibodies as a control to demonstrate equal amounts of cell lysate. Maximal expression levels of dyn^{wt} and dyn^{ts} were observed 3–4 d after removal of tetracycline and daily replacement of the culture medium. (B) dyn^{wt}- or dyn^{ts}-expressing cells were preincubated for 30 min at either 25 or 38°C and directly thereafter incubated in the presence of ^{125}I-Tf at the same temperature for the indicated times. Internalized ^{125}I-Tf was expressed as a percentage of total cell-associated ^{125}I-Tf (n = 2 ± SD). The results shown are representative of three independent experiments. In comparison with dyn^{wt} cells (○), uptake of ^{125}I-Tf by dyn^{ts} cells (□) was strongly reduced at 38°C but not at 25°C.

some-associated clathrin-coated buds by whole mount immunoelectron microscopy. HeLa cells were incubated with Tf/HRP for 1 h at 37°C to load the entire endocytic tract of the TfR with peroxidase activity. The cells were then incubated at 0°C in the presence of DAB, which polymerized in HRP-containing endosomes. Ascorbic acid, a membrane-impermeable agent, was also present during this incubation to prevent DAB polymerization at the plasma membrane or in deeply invaginated pits that are continuous with the plasma membrane. DAB polymer selectively fixed the endosomes and also served as an electron-dense marker for endosomes. Cytosolic proteins, including nonmembrane-associated dynamin, were removed after permeabilizing the plasma membrane with saponin. The resulting electron-lucent cells were then fixed with aldehydes, immunolabeled with colloidal gold, and studied as whole mount preparations using transmission electron microscopy. All endosomal tubules were decorated with buds that labeled heavily for both clathrin and endogenous dynamin-2 (Figure 1, for quantification see Figure 9A). The clathrin/dynamin-decorated endosomal tubules were not only found in the perinuclear area but also in the periphery of the cell. The peripheral endosomal tubules occasionally associated with vacuolar sorting endosomes. These observations suggest a role for endogenous dynamin-2 in the formation of clathrin-coated vesicles from endosomes.

TfR Recycling Is Inhibited by dyn^{ts}

To study the requirement for dynamin in TfR recycling we used HeLa cell lines that were previously established by the group of Dr. Schmid (Damke *et al.*, 1995a). These cells overexpress either a HA-tagged human dyn^{ts} or, as a control, HA-tagged dyn^{wt}. The expression of these constructs is under control of a tetracycline-regulatable chimeric transcription activator. When the cells were cultured at 32°C in the absence of tetracycline, dyn^{ts} was expressed within days but had only minor effects on dynamin-dependent processes at this temperature. However, within 5–10 min at 38°C, overexpressed dyn^{ts} strongly inhibited TfR uptake (Damke *et al.*, 1995a). Consistent with observations by Damke *et al.* (1995a), we observed that dyn^{wt} or dyn^{ts} were expressed only upon removal of tetracycline from the culture medium (Figure 2A). In our hands dyn^{wt} and dyn^{ts} were expressed homogeneously (van Dam and Stoorvogel, unpublished results) and at high levels (Figure 2A) only when the tissue culture medium was refreshed daily after removal of tetracycline. A control protein, tubulin, was equally expressed irrespective of the presence of tetracycline. For all further experiments, cells were cultured for 3–4 d at 32°C in the absence of tetracycline during which the culture medium was refreshed daily. Consistent with observations by Damke *et al.* (1995a), uptake of TfR by dyn^{ts}-expressing cells was strongly inhibited at 38°C (Figure 2B). TfR uptake was slightly inhibited at 30°C (van Dam and Stoorvogel, unpublished results), but at 25°C we observed no significant effect of dyn^{ts} on TfR uptake (Figure 2B).

Next, we focused on the effects of dyn^{ts} on TfR recycling. Cells were incubated for 60 min in the continuous presence of ^{125}I-Tf at either 25 or 38°C to load endosomes. ^{125}I-Tf was then dissociated from plasma membrane TfR using an acid-neutral wash procedure at 0°C (see MATERIALS AND METHODS). Clathrin-coated pits that accumulated at 38°C at the plasma membrane of dyn^{ts} cells were freely accessible for macromolecules (Damke *et al.*, 1995a; Baba *et al.*, 1999) and were thus emptied from ^{125}I-Tf by this procedure (see also below). Although ^{125}I-Tf was inefficiently endocytosed by dyn^{ts}-expressing cells at 38°C, the amount of intracellular label sufficed for recycling measurements. Recycling of en-

docytosed ^{125}I-Tf into the medium was measured during a reincubation of the cells at either 25 or 38°C. As expected, dyn^{ts} had no significant effect on ^{125}I-Tf recycling at 25°C (Figure 3A; Table 1). In contrast, at 38°C dyn^{ts} cells retained ~30% of previously endocytosed ^{125}I-Tf versus ~10% by dyn^{wt} cells, whereas the rate of recycling was not significantly affected (Figure 3B; Table 1).

To exclude the possibility that the inhibitory effect of dyn^{ts} on ^{125}I-Tf recycling was a secondary effect as a consequence of reduced uptake of either TfR or other membrane proteins that are essential for ^{125}I-Tf recycling, an alternative approach was taken in which cells were loaded with ^{125}I-Tf at 16°C, a temperature that is permissive for ^{125}I-Tf-uptake by dyn^{ts} cells. Other studies demonstrated that at 16°C TfR accumulates in sorting endosomes (Ren *et al.*, 1998, and references therein). Following loading at 16°C and removal of cell surface associated ^{125}I-Tf at 0°C, cells were incubated at either 25 or 38°C to allow recycling. As expected, at 25°C, ^{125}I-Tf recycling did not significantly differ between dyn^{wt}- and dyn^{ts}-expressing cells (Figure 3C; Table 1). However, at 38°C, also in this experimental setup, ~29% of previously endocytosed ^{125}I-Tf was retained by dyn^{ts}-expressing cells (Figure 3D; Table 1).

To further exclude the possibility that retention of ^{125}I-Tf by dyn^{ts} cells was reflecting an accumulation in dyn^{ts}-stabilized clathrin-coated pits at the plasma membrane, we performed an experiment in which cells were loaded with ^{125}I-Tf-SS-biotin. After recycling, cells were incubated at 0°C in the presence of MESNA, a membrane-impermeable reducing agent that removed biotin from surface exposed but not from intracellular ^{125}I-Tf-SS-biotin. The cells were then lysed, and nonreduced ^{125}I-Tf-SS-biotin was recovered from the cell lysates and the release media with immobilized streptavidin. With this approach we confirmed that at 38°C dyn^{ts} cells truly retained ~30% of the label intracellularly (Figure 3E; Table 1).

Only apo-Tf is efficiently released from recycling TfR, and dissociation of Fe^{3+} from Tf in endosomes is dependent on endosome acidification. A potential explanation for the results above could be that a proportion of ^{125}I-Tf failed to dissociate from recycling TfR in dyn^{ts} cells because of interference with endosome acidification. Although the data in Figure 3D already argued against this possibility, we performed experiments in which ^{125}I-Tf-loaded cells were washed at 0°C with an acetate buffer instead of an MES buffer. Both pH 5 buffers removed Fe^{3+} from ^{125}I-Tf at the plasma membrane with equal efficiency, but acetate, in contrast to MES, diffuses into cells and acidifies the weakly buffered lumen of endosomes. Consequently, treatment of cells at 0°C with acetate results in dissociation of Fe^{3+} from endosomal ^{125}I-Tf irrespective of vacuolar proton pump activity (van Weert *et al.*, 1995). To demonstrate the effectiveness of this protocol, a control experiment was performed in which the vacuolar proton pump in dyn^{wt} cells was inhibited with concanamycin A. As expected, concanamycin A strongly inhibited the release of ^{125}I-Tf from recycling TfR when the cells were first treated with MES buffer. This effect was, however, largely rescued when the MES buffer was replaced by acetate buffer (Figure 4B). The remaining, acetate resistant, effect of concanamycin A on ^{125}I-Tf recycling was due to impaired TfR recycling (van Weert *et al.*, 1995; Presley *et al.*, 1997). The acetate treatment itself did not affect

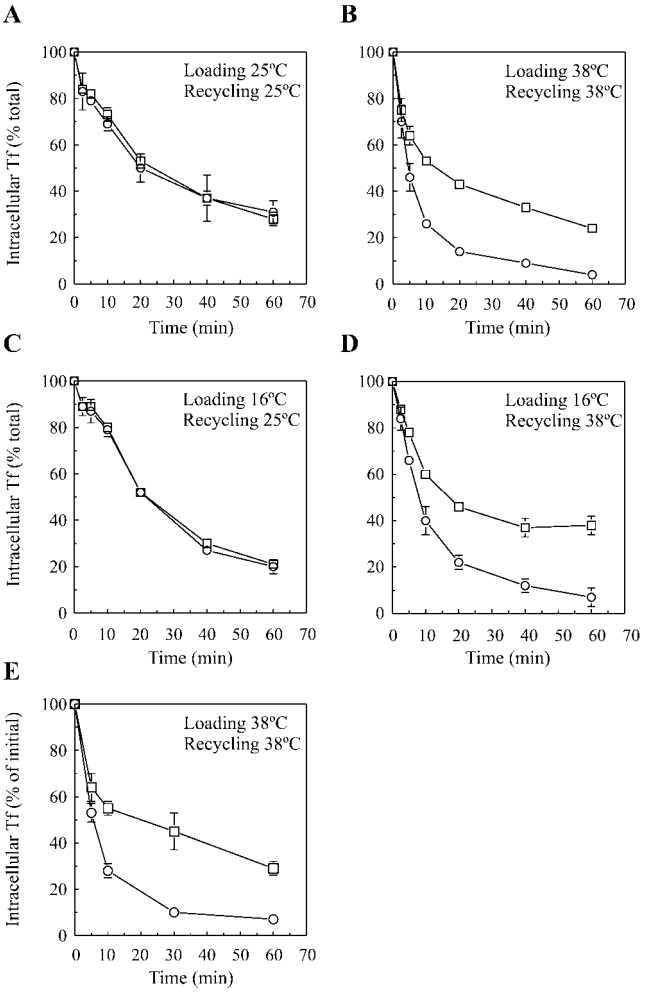

Figure 3. Inhibited TfR recycling by dyn^{ts}. (A and B) dyn^{wt} (○) and dyn^{ts} (□)-expressing cells were loaded with ^{125}I-Tf for 1 h at either 25°C (A) or 38°C (B). Cell surface-associated ^{125}I-Tf was removed at 0°C, after which recycling of endocytosed ^{125}I-Tf was measured during continued incubations at 25°C (A) or 38°C (B). Intracellular ^{125}I-Tf is plotted as a percentage of total endocytosed ^{125}I-Tf (n = 2, mean ± SD). The experiments shown are representative of 13 independent experiments, each with duplicate samples. For kinetic analysis, see Table 1. (C and D) Sorting endosomes of dyn^{wt} (○) and dyn^{ts} (□)-expressing cells were loaded with ^{125}I-Tf for 1 h at 16°C. Cell surface-associated ^{125}I-Tf was removed at 0°C, and recycling of endocytosed ^{125}I-Tf was measured at either 25°C (C) or 38°C (D). Intracellular ^{125}I-Tf is plotted as a percentage of total endocytosed ^{125}I-Tf (n = 2, mean ± SD). The experiments shown are representative of two to five independent experiments, each with duplicate samples. For the kinetic analysis, see Table 1. (E) dyn^{wt} (○) and dyn^{ts} (□)-expressing cells were loaded with ^{125}I-Tf-SS-biotin for 1 h at 38°C. Cell surface-associated ^{125}I-Tf-SS-biotin was removed at 0°C, after which recycling of endocytosed ^{125}I-Tf-SS-biotin was allowed at 38°C for the times indicated. The biotin moiety was then removed selectively from surface-exposed ^{125}I-Tf-SS-biotin by exposing the cells to MESNA at 0°C. Intracellular ^{125}I-Tf-SS-biotin was then collected from cell lysates and plotted as a percentage of total internalized ^{125}I-Tf-SS-biotin (mean ± SD from two independent experiments). For the kinetic analysis, see Table 1.

Table 1. Summary of kinetic parameters of ^{125}I-Tf recycling

	y_0 dyn^{wt}	y_0 dyn^{ts}	b dyn^{wt}	b dyn^{ts}	R^2 dyn^{wt}	R^2 dyn^{ts}	n	Figure
Load 25°C Chase 25°C	23.2 ± 6.3	24.5 ± 6.4	0.05 ± 0.01	0.05 ± 0.01	0.99 ± 0.01	0.99 ± 0.01	13	3A
Load 25°C Chase 25°C + BFA	38.8 ± 1.8	47.7 ± 1.1	0.05 ± 0.00	0.04 ± 0.01	0.96 ± 0.03	0.96 ± 0.02	2	10A
Load 38°C Chase 38°C	9.8 ± 3.9	29.9 ± 4.3	0.13 ± 0.02	0.12 ± 0.03	0.99 ± 0.00	0.96 ± 0.00	13	3B
Load 38°C Chase 38°C + BFA	17.9 ± 2.6	31.3 ± 9.2	0.09 ± 0.01	0.12 ± 0.04	0.98 ± 0.00	0.93 ± 0.06	2	10B
Load 16°C Chase 25°C	11.7 ± 7.0	15.4 ± 1.3	0.04 ± 0.00	0.03 ± 0.01	0.99 ± 0.00	0.97 ± 0.02	2	3C
Load 16°C Chase 38°C	8.1 ± 5.2	29.3 ± 12.8	0.10 ± 0.01	0.08 ± 0.02	1.0 ± 0.00	0.98 ± 0.01	5	3D
^{125}I-Tf-SS-biotin Load 38°C Chase 38°C	7.2 ± 1.0	36.3 ± 7.0	0.15 ± 0.02	0.15 ± 0.05	1.0 ± 0.00	0.94 ± 0.06	2	3E

Kinetic parameters were obtained by fitting data points into single exponential decay equations with three parameters, $y = y_0 + a.e^{bt}$. The amount of retained ^{125}I-Tf, y_0, is expressed as a percentage of total internalized ^{125}I-Tf, the rate of ^{125}I-Tf recycling (min^{-1}) by b. R^2, the coefficient of determination, is an indication for the fit of the calculated curves and equals 1 for ideally fitting curves. The tolerance of the obtained values was satisfactory. Double exponential decay equations with five parameters yielded irreproducible values and therefore were not appropriate for curve fitting. Numbers are means ± SD from n experiments, each in duplicate. For experiments with ^{125}I-Tf-SS-biotin, two independent experiments with single samples were performed.

the release of ^{125}I-Tf by dyn^{wt} cells (Figure 4A). Most importantly, the kinetics of ^{125}I-Tf release by acetate- and MES-treated dyn^{ts} cells were the same (Figure 4A), confirming that retention of ^{125}I-Tf by dyn^{ts} cells was not due to interference with endosome acidification.

Tf Is Retained by Recycling Endosomes in dyn^{ts} Cells

To study the overall effect of dyn^{ts} on the distribution of TfR-containing endosomes, dyn^{wt}- and dyn^{ts}-expressing cells were incubated at 38°C for 30 min, fixed, immunodouble–labeled for dynamin-1 and TfR and examined by confocal laser scanning microscopy (Figure 5). Consistent with other reports (Damke *et al.*, 1995a; Baba *et al.*, 1999), dyn^{wt} and dyn^{ts} distributed diffusely throughout the cell, whereas dyn^{ts} also was concentrated in large intracellular aggregates as well as at the plasma membrane. In dyn^{ts} cells TfR labeling was more pronounced at the plasma membrane and in the perinuclear area compared with dyn^{wt} cells. In addition, TfR-labeled endosomes had a more tubular appearance in dyn^{ts} cells than in dyn^{wt} cells, and some dyn^{ts} seemed to associate with these tubules.

To determine the subcellular site at which endocytosed Tf accumulated, cells were pulse-labeled for 1 h at 38°C with TaR-Tf and a fluid-phase endocytic marker, F-dextran (Figure 6). After 1 h of uptake, extracellular labels and plasma membrane-associated TaR-Tf were removed at 0°C and cells were then either fixed directly or chased for 1 h at 38°C before fixation. In dyn^{wt} cells, F-dextran and TaR-Tf localized after uptake mostly to distinct endocytic structures, indicating rapid and efficient sorting of these markers into late endosomes/lysosomes and recycling endosomes, respectively (Figure 6, A–C). Similar observations were made for dyn^{ts} cells (Figure 6, G–I), indicating that the exit of TfR from sorting endosomes into recycling endosomes was not affected. After a 60-min chase, dyn^{wt} cells released almost all endocytosed TaR-Tf, whereas F-dextran remained intracellularly (Figure 6, D–F). In contrast, dyn^{ts} cells retained a significant amount of TaR-Tf in F-dextran-lacking compartments after a 60-min chase (Figure 6, J–L). To characterize these compartments, dyn^{ts} cells were pulse-labeled with TaR-Tf, chased, fixed, and immunolabeled for TGN46, a marker for TGN (Prescott *et al.*, 1997), or for EEA1, a marker specific for sorting endosomes (Mu *et al.*, 1995). TaR-Tf that accumulated in the perinuclear area did not codistribute with TGN46 (Figure 7, top row), indicating that TaR-Tf was not mistargeted to or retained at the TGN. TaR-Tf also did not codistribute with EEA1 (Figure 7, bottom row), confirming that transport from sorting endosomes to recycling endosomes was not affected. Recycling endosomes originally have been defined by the kinetics with which they are loaded and emptied from endocytosed Tf as well as by their perinuclear location. Other molecular markers that exclusively label this compartment have not been described to date. In dyn^{ts} cells, we observed only little overlap of pulse-chased TaR-Tf with cellubrevin and Rab11 (van Dam and Stoorvogel, unpublished results), consistent with the notion that these molecules only partially associate with recycling endosomes (see, for example Teter *et al.*, 1998; Sönnichsen *et al.*, 2000; Wilcke *et al.*, 2000, and references therein). Collectively, our data indicate that dyn^{ts} cells accumulated TaR-Tf in recycling endosomes.

dyn^{ts} Accumulates on Endosomal Clathrin-coated Buds

To study the effects of dyn^{ts} on endosomes in more detail, we took advantage of the whole mount approach as described above. In dyn^{wt}-expressing cells, only little, if any, dyn^{wt} was found associated with DAB-positive endosomal

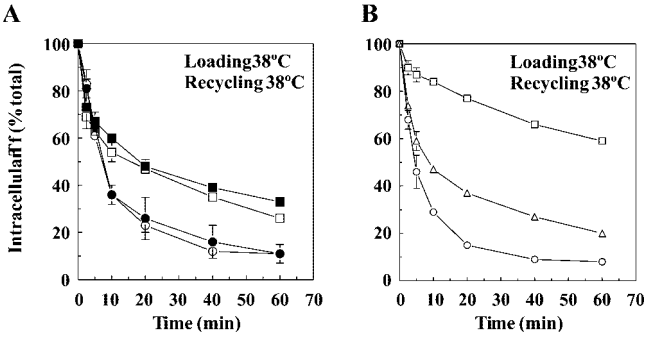

Figure 4. Inhibition of Tf recycling by dyn^{ts} is not due to defective endosome acidification. (A) dyn^{wt} (circles) and dyn^{ts} (squares)-expressing cells were loaded with ^{125}I-Tf for 1 h at 38°C. Cell surface-associated ^{125}I-Tf was removed at 0°C by the acidic-neutral wash procedure using either MES buffer (open symbols) or acetate buffer (closed symbols). The cells were then reincubated at 38°C, and the release of ^{125}I-Tf was measured. Intracellular ^{125}I-Tf is plotted as a percentage of total endocytosed ^{125}I-Tf (n = 2, mean ± SD). The experiments shown are representative of three independent experiments, each with duplicate samples. The acetate treatment assured the release of Fe^{3+} from intracellular ^{125}I-Tf. dyn^{ts} inhibited the release of ^{125}I-Tf irrespective of acetate or MES treatment. Lack of endosome acidification thus can not explain the results. (B) As a positive control for this procedure, dyn^{wt}-expressing cells were loaded for 1 h at 38°C with ^{125}I-Tf in the absence (○) or presence (△ and □) of 100 nM of concanamycin A, a vacuolar proton pump inhibitor. Cell surface-associated ^{125}I-Tf was removed at 0°C by the acid-neutral wash procedure using either MES buffer (□) or acetate buffer (○ and△). Cells were then reincubated at 38°C in the absence (○) or presence (△ and □) of 100 nM concanamycin A and release of ^{125}I-Tf was measured. Intracellular ^{125}I-Tf is plotted as a percentage of total internalized ^{125}I-Tf. The results shown (n = 2, mean ± SD) are representative of five independent experiments. The acetate treatment restored ^{125}I-Tf recycling by concanamycin A-treated cells, illustrating the effectiveness of this procedure.

tubules (Figure 8, A and C) and <10% of endosome-associated clathrin-coated buds labeled for dyn^{wt} (Figure 8A). In contrast, a significant amount of dyn^{ts} was associated with endosomal clathrin-coated buds (Figure 8, B and D). Consistent with the fluorescent images (Figure 5), in dyn^{ts} cells endosomal tubules increased in length, and the number of clathrin-coated buds per endosome was amplified more than fivefold compared with dyn^{wt} cells. dyn^{ts}/clathrin-labeled tubules were encountered in the perinuclear area, but they were also abundant at the periphery of the cell. Most endosomal tubules were not continuous with vacuolar sorting endosomes, thus classifying them as recycling endosomes. Almost all endosome-associated buds labeled for both clathrin and dyn^{ts} (Figures 8B and 9B), suggesting that dyn^{ts} interfered with pinching off of clathrin-coated vesicles from recycling endosomes. To exclude that these clathrin-coated buds were derived from the plasma membrane, preparations were double-labeled for dynamin-1 and AP-2, an adaptor protein complex that associates with plasma membrane-derived clathrin-coated vesicles. AP-2 was virtually absent on endosomes (Stoorvogel *et al.*, 1996). As a positive control, the DAB incubation was performed in the absence of ascorbic acid, thus allowing DAB polymerization in clathrin-coated pits at the plasma membrane. Using this procedure we detected many DAB-positive 100-nm vesicles/buds that labeled for clathrin, dynamin-1, and AP-2, but these were not associated with endosomes (Stoorvogel *et al.*, 1996). dyn^{ts}-containing recycling endosomes labeled heavily for TfR (Figure 8D). Endosome-associated clathrin-coated buds also contained TfR as indicated by experiments in which the coats, which impose stearic hindrance for TfR labeling, were stripped from DAB-filled endosomes with 0.5 M Tris before aldehyde fixation (Stoorvogel *et al.*, 1996). Together with the observation that endogenous dynamin-2 associates with clathrin-coated buds on endosomes (Figures 1 and 9A), these data strongly suggest that clathrin-coated vesicles pinch off from recycling endosomes in a dynamin-dependent manner.

BFA Interferes with the Dynamin-dependent TfR-recycling Pathway

BFA induces the formation of long endosomal tubules, possibly as a result of inhibited clathrin-coated vesicle formation at endosomes (Stoorvogel *et al.*, 1996). When clathrin-coated vesicles play a role in TfR recycling, BFA and dyn^{ts} should interfere with the same pathway. To test this hypothesis, cells were pulse-labeled with ^{125}I-Tf in the absence of BFA and chased in the presence of BFA (Figure 10; Table 1). At 25°C, both dyn^{ts} and dyn^{wt} cells retained significant amounts of ^{125}I-Tf in the presence of BFA (~39–48%) consistent with a requirement of clathrin-coated vesicles for efficient TfR recycling. At 38°C, the amount of ^{125}I-Tf retained by dyn^{wt} cells was also significantly increased by BFA (~18%), although the majority recycled with unchanged kinetics. The loss of a clathrin-mediated recycling pathway in the presence of BFA may have been compensated in part by an alternative BFA-insensitive pathway or mechanism. In contrast, in dyn^{ts} cells, stable clathrin-coated buds on endosomes were already formed during loading in the absence of BFA. When such stable coated buds retain a significant amount of intracellular TfR, ^{125}I-Tf recycling cannot be compensated via alternative pathway(s), not even in the presence of BFA. Consistent with this notion, BFA did not change the efficiency of ^{125}I-Tf recycling by dyn^{ts} cells at 38°C (retention of ~31 vs. ~30%).

Taken together our data indicate that endosome-derived clathrin-coated vesicles play a role in the endosomal recycling pathway and that endocytosed TfR is, at least in part, recycled via this pathway. Although we did observe TfR in endosome-associated clathrin-coated buds, we have been unable to determine whether TfR is concentrated in these buds. Thus, the question whether TfR is actively or passively recruited into these vesicles remains to be answered.

DISCUSSION

Tubular endosomes are abundantly covered with TfR-containing clathrin-coated buds (Stoorvogel *et al.*, 1996). Here we demonstrate that these buds, like clathrin-coated pits at the plasma membrane, carry endogenous dynamin-2. Furthermore, we show that exogenously expressed dyn^{ts} accumulated at clathrin-coated buds on recycling endosomes and interfered with TfR recycling. BFA interfered with the assembly of clathrin coats on endosomes and, like dyn^{ts}, reduced the extent of Tf recycling. BFA had no additive effect on Tf recycling by dyn^{ts} cells, consistent with the

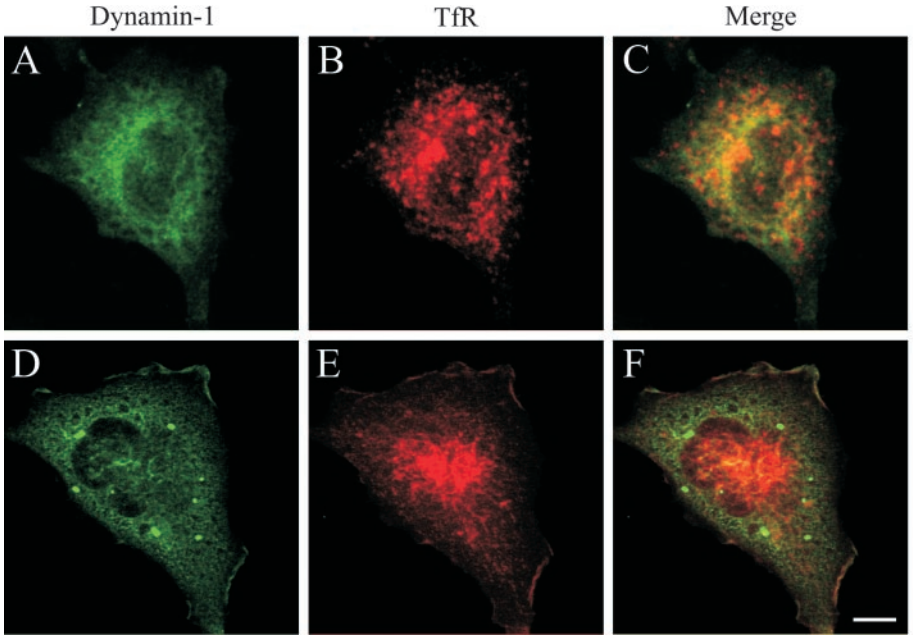

Figure 5. dyn^{ts} cells redistribute intracellular TfR. dyn^{wt} (A–C) and dyn^{ts} (D–F)-expressing cells were incubated for 30 min at 38°C, fixed, and immuno-double–labeled for dynamin-1 (green) and TfR (red). Integrated views of entire cells were obtained by superimposition of 25 sequential 0.3-μm optical sections. Note that in dyn^{ts} cells dynamin-1 accumulated at the edge of the cell and in large aggregates. TfR accumulated at the plasma membrane as well as in tubular endosomes in the perinuclear area. The latter structure apparently also accumulated dyn^{ts}. Bar, 10 μm.

notion that TfR egresses recycling endosomes, at least in part, by endosome-derived clathrin-coated vesicles in a dynamin-dependent manner.

The inhibitory effect of dyn^{ts} on TfR recycling is direct and not an indirect consequence of decreased membrane uptake. The first argument is that, although dyn^{ts} interfered with clathrin-mediated uptake of TfR, endocytosis of total membrane remained unaffected because of up-regulated alternative pathways (Damke *et al.*, 1995a). Thus, the flow of membrane into endosomes was not affected. Second, dyn^{ts} also interfered with recycling at 38°C when ^{125}I-Tf was first endocytosed at 16°C, a temperature that is permissive for the uptake of TfR and other membrane constituents (Figure 3D; Table 1). This experiment also excludes the possibility that intracellular retention of TfR was due to the depletion of membrane protein(s) from endosomes that are essential for recycling. Third, dynamin-1^{K44A} interfered with TfR uptake but not with recycling (Altschuler *et al.*, 1998), demonstrating that these processes can be uncoupled. Fourth, BFA interfered with TfR recycling by dyn^{wt} cells but had no additional inhibitory effect on dyn^{ts} cells at 38°C (Figure 10; Table 1), suggesting that dyn^{ts} inhibited TfR recycling downstream of the BFA-sensitive step. Because BFA prevented the formation of clathrin-coated buds at endosomes but not at the plasma membrane, interference with TfR recycling by dyn^{ts} can be explained only by a direct effect on endosomes. Finally, we demonstrated the presence of endogenous dynamin-2 as well as dyn^{ts} on clathrin-coated buds on endosomes (Figures 1, 8, B and D, and 9).

Depending on the experimental protocol, dyn^{ts}-expressing cells retained 29–36%of internalized ^{125}I-Tf at the nonpermissive temperature (Figure 3). From these data it cannot be concluded whether all or just part of endocytosed TfR recycles via a dynamin-dependent pathway. A proportion of endocytosed ^{125}I-Tf might have leaked through the dyn^{ts}-induced block in the recycling pathway, similar to what has been observed for the effect of dyn^{ts} on clathrin-mediated endocytosis (Damke *et al.*, 1995a; Figure 2B). In addition, it should be noted that cells had to be incubated at 0°C in between loading with ^{125}I-Tf and the chase to remove cell surface-associated ^{125}I-Tf. When the temperature was elevated to 38°C to allow recycling, a proportion of endocytosed ^{125}I-Tf might have been transported beyond the dynamin-dependent step before the dyn^{ts}-imposed block became maximally effective. This is a likely explanation because TfR is transferred from sorting endosomes into the recycling pathway within minutes after uptake (Stoorvogel *et al.*, 1987), whereas the inhibitory effect of dyn^{ts} is maximal only after 5–20 min at 38°C (Damke *et al.*, 1995a). In ^{125}I-Tf uptake experiments, maximal inhibitory effects of dyn^{ts} were obtained only after a preincubation at the nonpermissive temperature (Figure 2B). Such an approach is technically impossible for recycling assays and because of these experimental limitations, the amount of TfR that recycles via a dynamin-dependent pathway might be underestimated. An alternative explanation for the partial interference of dyn^{ts} with TfR recycling could be the existence of two parallel recycling pathways or mechanisms, of which only one is sensitive to dyn^{ts}. Currently we cannot discriminate between these possibilities.

In contrast to this study, others reported that TfR recycling occurs independently of dynamin and clathrin function. These conclusions were based on the observations that K44A, K694A, and R725A dynamin mutants (Damke *et al.*, 1994; Altschuler *et al.*, 1998; Sever *et al.*, 2000) and the clathrin Hub domain (Bennett *et al.*, 2001) did not severely affect TfR recycling. We also studied TfR trafficking in dynamin-1^{K44A}-expressing cells and confirmed that TfR recycling was not affected to the same extent as in dyn^{ts}-expressing cells (van Dam and Stoorvogel, unpublished results). This controversy can be explained when constitutive suppression of the clathrin-dependent recycling pathway results in up-regulated compensatory alternative, clathrin-independent, recycling pathway(s) or mechanism(s). This scenario is plau-

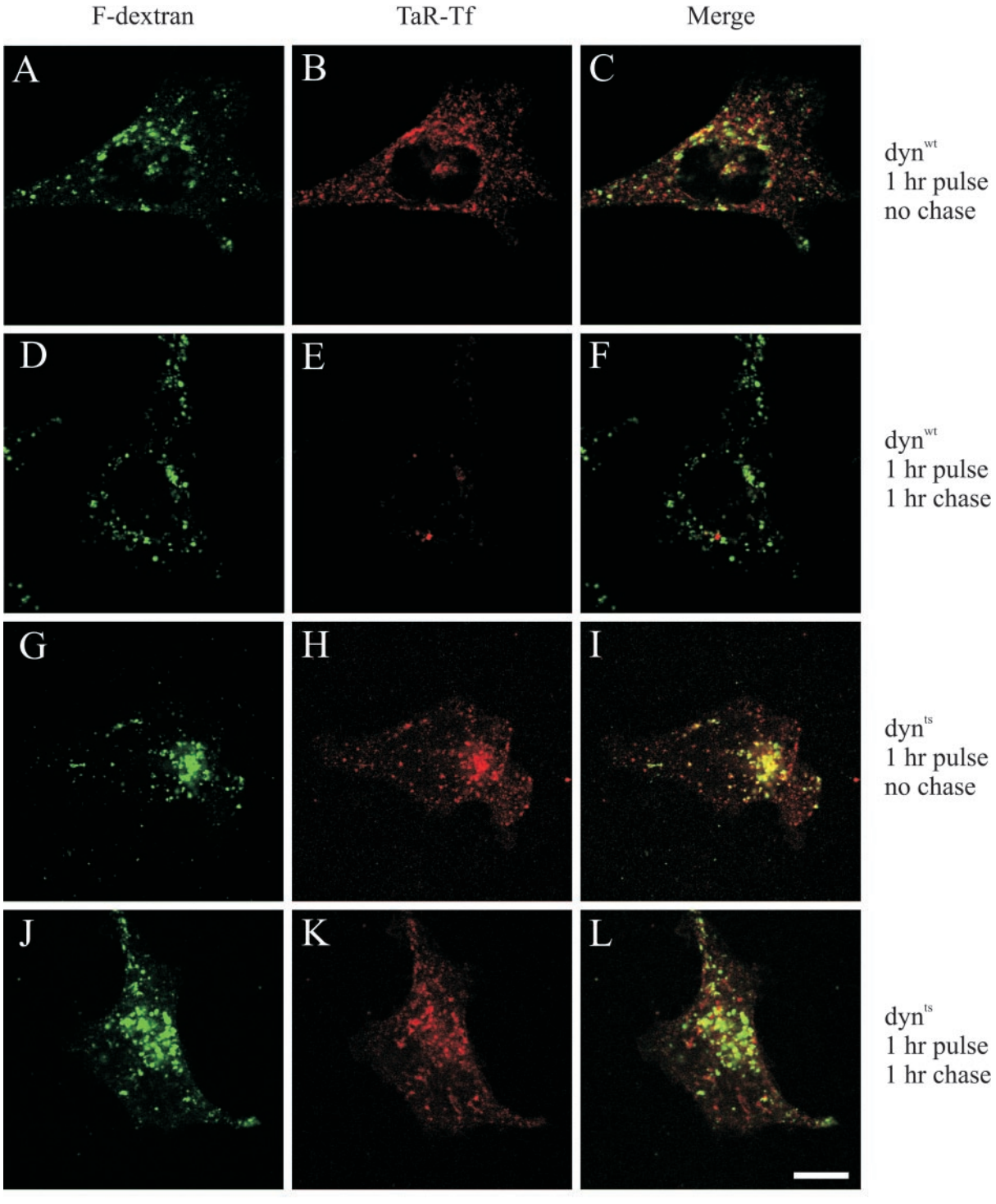

Figure 6. dyn^{ts} cells accumulate endocytosed Tf in a perinuclear compartment. dyn^{wt} (A–F) and dyn^{ts} (G–L)-expressing cells were pulse-labeled with both TaR-Tf and F-dextran for 1 h at 38°C. Extracellular and cell surface-associated labels were removed at 0°C by the acid-neutral wash procedure. The cells were then either fixed immediately (A–C, G–I) or chased for 1 h at 38°C before fixation (D-F, J-L). dyn^{wt} cells released almost all TaR-Tf during the chase, whereas dyn^{ts} cells retained significant amounts of TaR-Tf in F-dextran lacking endosomes that localize both at the perinuclear area and at the periphery of the cell. Bar, 10 μm.

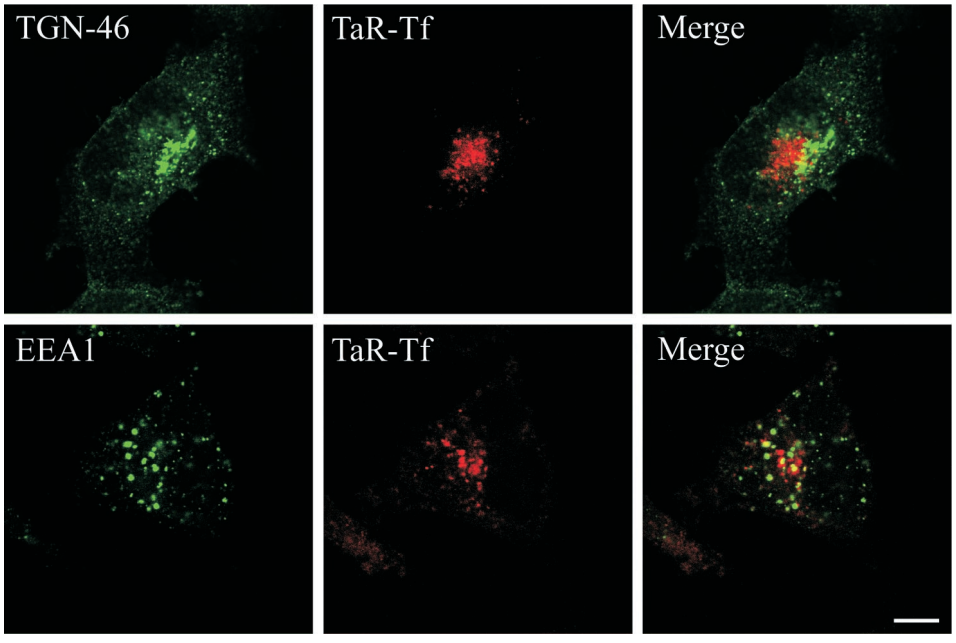

Figure 7. dyn^{ts} cells accumulate Tf in recycling endosomes. dyn^{ts}-expressing cells were loaded with TaR-Tf for 1 h at 38°C. Cell surface-associated TaR-Tf was removed at 0°C by the acid-neutral wash procedure and the cells were chased for 1 h at 38°C, fixed, permeabilized, and immunolabeled for either TGN-46 or EEA1. TaR-Tf was retained in peripheral and perinuclear endosomes that are distinct from the TGN (TGN-46) and sorting endosomes (EEA1). Bar, 10 μm.

sible because cells have been demonstrated to up-regulate alternative routes to compensate for loss of dynamin-dependent pathways. For example, transfer of dyn^{ts}-expressing cells to 38°C initially resulted in a 50% reduction in fluid-phase uptake because of blocked clathrin-mediated endocytosis. After 30 min, however, this defect was fully compensated by up-regulated dyn^{ts}-insensitive non-clathrin-dependent endocytic pathway(s) (Damke *et al.*, 1995a). Similarly, constitutive defects in the clathrin-mediated recycling pathway may be compensated by parallel recycling pathway(s) or mechanisms. In this respect, it is important to realize that the turnover of early endosomal membranes is much faster than that of the plasma membrane (McVey Ward *et al.*, 1995, and references therein) and that interference with one of two or more parallel recycling pathways might have limited consequences for recycling kinetics. Induction of parallel recycling pathways or mechanisms would also be consistent with the profound intracellular redistribution of TfR in cells overexpressing the dominant-negative clathrin Hub fragment (Bennett *et al.*, 2001).

The whole mount immunoelectron microscopy described here is suitable only to detect endosome-associated antigens. Using immunoelectron microscopy on cryosections, we detected dynamin-2 on clathrin-coated pits at the plasma membrane and clathrin buds on TfR-containing endosomes, as well as on other unidentified intracellular membranes (van Dam and Stoorvogel, unpublished results). Using the same technique and cell lines, others reported the association of dynamin-2 with tubulovesicular appendices on late endosomes and retention of cation-independent mannose 6-phosphate receptor in this compartment in cells that overexpress dynamin-1^{K44A} (Nicoziani *et al.*, 2000). Late endosomal dynamin-2–labeled structures did not contain clathrin, consistent with the notion that cation-independent mannose 6-phosphate receptor trafficking from late endosomes to the TGN does not seem to require clathrin (Draper *et al.*, 1990). Dynamin has also been localized at the TGN, and its involvement in budding of clathrin-coated and other vesicles from this compartment has been reported (Henley and McNiven, 1996; Maier *et al.*, 1996; Cao *et al.*, 1998; Jones *et al.*, 1998). Thus, multiple clathrin-dependent and -independent intracellular transport pathways require dynamin function, and the TfR-recycling pathway described here adds to this list.

With the exception of polarized cells (Sheff *et al.*, 1999), recycling of endocytosed Tf generally can be described with single exponential kinetics ($t_{1/2} \sim 9$–12 min; Mayor *et al.*, 1993, and references therein; Table 1). dyn^{ts} interfered with the extent but not with the rate of ^{125}I-Tf recycling. Thus, two recycling pathways with one being inhibited by dyn^{ts} can be accommodated only when they display similar kinetics. Morphological evidence indicates that sorting endosomes are rapidly emptied from endocytosed Tf ($t_{1/2} \sim 5$ min), whereas recycling endosomes retain Tf much longer ($t_{1/2} \sim 15$–30 min). Sorting endosome-derived Tf may be transported to the plasma membrane either directly or indirectly via the perinuclear recycling endosomes (Yamashiro *et al.*, 1984; Daro *et al.*, 1996; Ullrich *et al.*, 1996; Sheff *et al.*, 1999). In such a dual pathway model it is possible that dyn^{ts} interfered only with the indirect recycling pathway because TaR-Tf accumulated predominantly in a perinuclear compartment with the characteristics of recycling endosomes (Figures 5–7). However, dynamin-2 and dyn^{ts} were not only observed on clathrin-coated buds on tubular endosomes in the perinuclear area but also on those in the periphery of the cell. Possibly, tubular recycling endosomes are already formed at the cell periphery when vacuolar sorting endosomes detach their tubular extensions. Peripherally formed tubular endosomes might then migrate along microtubules to the perinuclear area where they accumulate as the so-called recycling compartment. In this latter model, the periphery of pulse-chase–labeled cells will be emptied from Tf more rapidly than the perinuclear area even when recycling occurs via a single pathway by first-order kinetics.

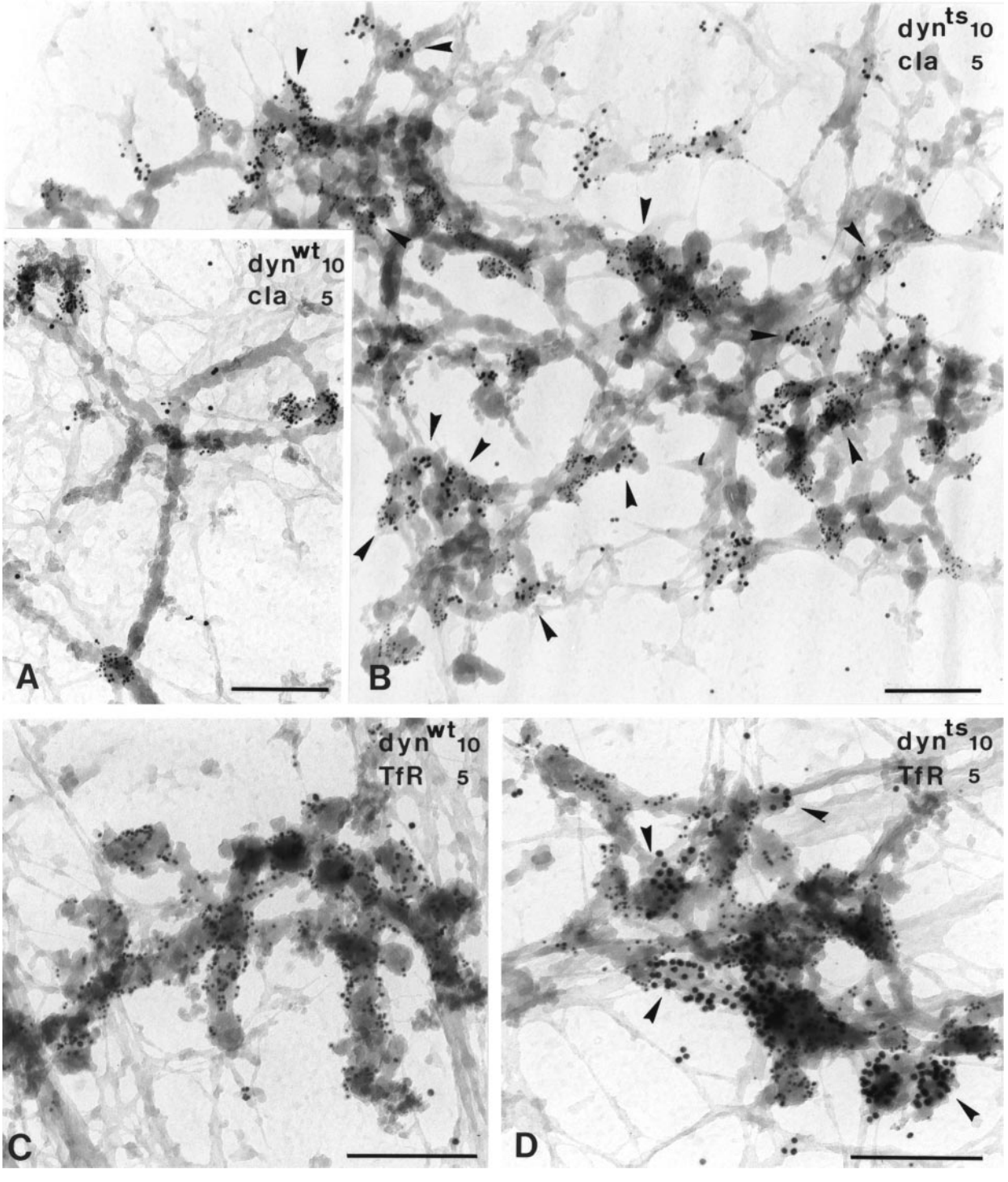

Figure 8. dyn^{ts} localizes on endosomal clathrin-coated buds. dyn^{wt} (A and C) and dyn^{ts} (B and D) cells were incubated for 1 h at 25°C with Tf/HRP to allow loading of the entire recycling pathway with HRP activity. The cells were then incubated for 5 min at 38°C to initiate the dominant-negative effect of dyn^{ts}. The cells were processed for whole mount immunoelectron microscopy and labeled for dynamin-1 (dyn^{wt} or dyn^{ts}, 10-nm gold) and clathrin (cla, 5-nm gold; A and B) or dynamin-1 (10-nm gold) and TfR (5-nm gold; C and D). (A) Clathrin-coated buds on tubular endosomes in dyn^{wt} cells are largely devoid of dyn^{wt}. (B) Clathrin-coated buds on extended tubular endosomal networks in dyn^{ts} cells are mostly labeled for dyn^{ts} (for examples, see arrowheads). For quantification, see Figure 9. (C) TfR-labeled tubular endosomes in dyn^{wt} cells contain little, if any, dyn^{wt}. (D) TfR-labeled endosomes in dyn^{ts} cells contain many dyn^{ts}-labeled buds (arrowheads). Limited labeling for TfR on dyn^{ts}-containing buds was probably due to stearic hindrance. Bars, 200 nm.

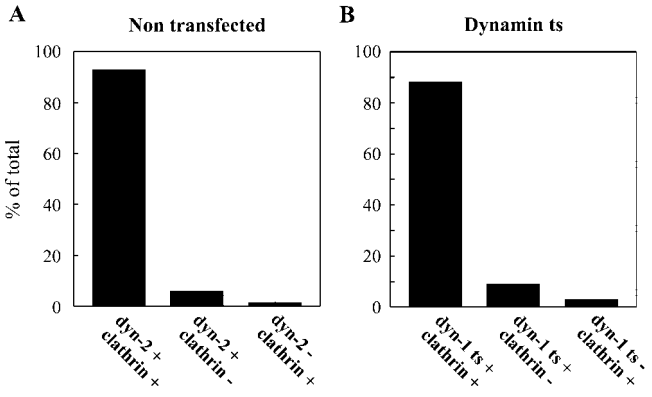

Figure 9. Dynamin and clathrin codistribute on endosomal buds. (A) Double-labeled whole mount immunoelectron microscopic preparations of nontransfected HeLa cells (see Figure 1) were analyzed for the presence of endogenous dynamin-2 and clathrin on endosomal buds. Of 300 immunolabeled DAB-positive buds that were counted, ~93% contained both endogenous dynamin-2 and clathrin. (B) Double-labeled whole mount immunoelectron microscopic preparations of dyn^{ts} cells (see Figure 8B) were analyzed for the presence of dyn^{ts} and clathrin on endosomal buds. Of 700 labeled DAB-positive buds that were counted, ~90% contained both dyn^{ts} and clathrin.

Maxfield and coworkers reported that a bulk-phase membrane marker and a TfR deletion mutant that lacked its cytoplasmic domain recycled with kinetics indistinguishable from wild-type TfR, and they concluded that sorting information is not required for TfR recycling (Johnson *et al.*, 1993; Mayor *et al.*, 1993). In this light it should be noted that we have not demonstrated that clathrin-coated buds in endosomes actively recruit TfR. TfR might be either actively or passively incorporated into clathrin-coated vesicles. Even tailless TfR should recycle almost quantitatively because, of all endocytosed membrane, ~95% is eventually recycled to the plasma membrane and only ~5% is targeted to lysosomes (Haylett and Thilo, 1986; Draye *et al.*, 1988). Active recruitment into the recycling pathway thus seems not to be required for a single round of endocytosis. However, with 5% mistargeting and 15-min iterative endocytic cycles, the half-life of the TfR would be reduced to a few hours only. To maintain a 1- to 2-d half-life, mistargeting to lysosomes should be reduced from 5 to 0.5% per cycle (Omary and Trowbridge, 1981). Endosome-derived clathrin-coated vesicles may be required to achieve such a high recycling efficiency. Single-cycle experiments do not discriminate between recycling efficiencies of 99.5 and 95%. Thus, the initial observations by Maxfield *et al.* do not exclude the possibility of active TfR recycling. In fact, in a later study, Maxfield and coworkers demonstrated that the vacuolar proton pump inhibitor bafilomycin interfered with recycling of wild-type TfR but not of TfRs that carried a mutation in their internalization signal or a deletion (Δ3–59) in their cytoplasmic domain (Johnson *et al.*, 1993; Presley *et al.*, 1997), indicating that sorting information is required for efficient TfR recycling under those conditions. Others demonstrated that recycling of internalized TfR to the basolateral plasma membrane of polarized cells requires information within residues 19–41 and that this sorting signal is distinct from the tyrosine-based internalization motif and the basolateral sorting motif in the biosynthetic pathway (Odorizzi and Trowbridge, 1997). Finally, it was recently demonstrated that dominant interfering mutants of Hsc70, a protein required for uncoating of clathrin-coated vesicles, interfered with TfR recycling (Newmyer and Schmid, 2001). Combined with these data, our observations suggest that TfR may be recruited actively into endosome-derived clathrin-coated recycling vesicles.

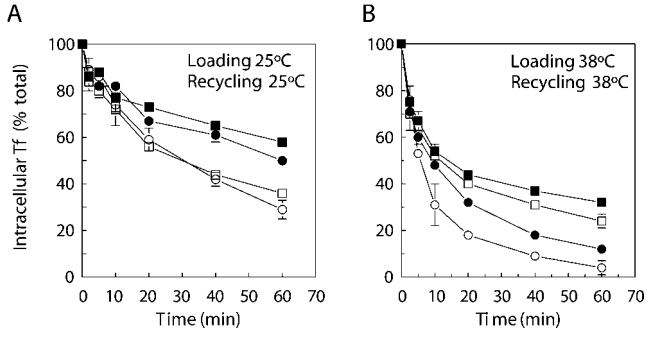

Figure 10. Interference of TfR recycling by BFA. (A and B) dyn^{wt} (circles) and dyn^{ts} (squares)-expressing cells were loaded with ^{125}I-Tf for 1 h at either 25°C (A) or 38°C (B). Cell surface-associated ^{125}I-Tf was removed at 0°C, and the cells were reincubated at 25°C (A) or 38°C (B) in the absence (open symbols) or presence (closed symbols) of 10 μg/ml BFA, and the release of ^{125}I-Tf was measured. Intracellular ^{125}I-Tf is plotted as a percentage of total endocytosed ^{125}I-Tf (n = 2, mean ± SD). The experiments shown are representative of two independent experiments each with duplicate samples. For the kinetic analysis see Table 1. At 25°C BFA interfered with ^{125}I-Tf recycling by both dyn^{wt} and dyn^{ts} cells. In contrast, at 38°C BFA had no additive effect on ^{125}I-Tf recycling by dyn^{ts} cells.

Although adaptor protein complexes that exclusively associate with endosomes have not yet been identified, we have previously demonstrated the presence of γ-adaptin (Stoorvogel *et al.*, 1996) and β3-adaptin (Dell Angelica *et al.*, 1998) on endosomal clathrin-coated buds. AP-1 and AP-3 adaptor protein complexes have no reported affinity for TfR. These adaptors may, however, contain alternative μ subunits with distinct specificities. For example, it has recently been demonstrated that in polarized cells AP-1 may contain either one of two different μ isoforms, μ1A or μ1B. Both function at the TGN, but whereas the first is important for transport to endosomes, the second is involved in transport to the basolateral plasma membrane (Fölsch *et al.*, 1999). Yet another μ isoform or even an unidentified novel adaptor complex may recruit TfR into clathrin-coated buds on endosomes. Alternatively, TfR may require a posttranslational modification, such as phosphorylation, for binding to endosome-associated adaptor complexes.

Collectively, our data indicate that endosome-derived clathrin-coated vesicles carry recycling TfR back to the plasma membrane and that this pathway is dependent on dynamin. Important issues that remain include the question whether these clathrin-coated vesicles actively recruit TfR and/or other membrane proteins and the identification of other components of the molecular machinery that drives this pathway.

ACKNOWLEDGMENTS

We thank Brigitte Groothuis and Karen Jansen for excellent technical assistance, René Scriwanek for photographic assistance, David James for valuable discussions and Dr. S.L. Schmid for providing the dynamin-1–expressing cell lines. This work was supported by a grant from The Netherlands Organization for Scientific Research.

REFERENCES

Altschuler, Y., Barbas, S.M., Terlecky, L.J., Tang, K., Hardy, S., Mostov, K.E., and Schmid, S.L. (1998). Redundant and distinct functions for dynamin-1 and dynamin- 2 isoforms. J. Cell Biol. *143*, 1871–1881.

Baba, T., Ueda, H., Terada, N., Fujii, Y., and Ohno, S. (1999). Immunocytochemical study of endocytotic structures accumulated in HeLa cells transformed with a temperature-sensitive mutant of dynamin. J. Histochem. Cytochem. *47*, 637–648.

Bennett, E.M., Lin, S.X., Towler, M.C., Maxfield, F.R., and Brodsky, F.M. (2001). Clathrin hub expression affects early endosome distribution with minimal impact on receptor sorting and recycling. Mol. Biol. Cell *12*, 2790–2799.

Cao, H., Garcia, F., and McNiven, M.A. (1998). Differential distribution of dynamin isoforms in mammalian cells. Mol. Biol. Cell *9*, 2595–2609.

Chin, D.J., Straubinger, R.M., Acton, S., Nathke, I., and Brodsky, F.M. (1989). 100-kDa polypeptides in peripheral clathrin-coated vesicles are required for receptor-mediated endocytosis. Proc. Natl. Acad. Sci. USA *86*, 9289–9293.

Damke, H., Baba, T., van der Bliek, A.M., and Schmid, S.L. (1995a). Clathrin-independent pinocytosis is induced in cells overexpressing a temperature-sensitive mutant of dynamin. J. Cell Biol. *131*, 69–80.

Damke, H., Baba, T., Warnock, D.E., and Schmid, S.L. (1994). Induction of mutant dynamin specifically blocks endocytic coated vesicle formation. J. Cell Biol. *127*, 915–934.

Damke, H., Gossen, M., Freundlieb, S., Bujard, H., and Schmid, S.L. (1995b). Tightly regulated and inducible expression of dominant interfering dynamin mutant in stably transformed HeLa cells. Methods Enzymol. *257*, 209–220.

Daro, E., van der Sluijs, P., Galli, T., and Mellman, I. (1996). Rab4 and cellubrevin define different early endosome populations on the pathway of transferrin receptor recycling. Proc. Natl. Acad. Sci. USA *93*, 9559–9564.

Dell Angelica, E.C., Klumperman, J., Stoorvogel, W., and Bonifacino, J.S. (1998). Association of the AP-3 adaptor complex with clathrin. Science *280*, 431–434.

Draper, R.K., Goda, Y., Brodsky, F.M., and Pfeffer, S.R. (1990). Antibodies to clathrin inhibit endocytosis but not recycling to the trans Golgi network in vitro. Science *248*, 1539–1541.

Draye, J.P., Courtoy, P.J., Quintart, J., and Baudhuin, P. (1988). A quantitative model of traffic between plasma membrane and secondary lysosomes: evaluation of inflow, lateral diffusion, and degradation. J. Cell Biol. *107*, 2109–2115.

Fölsch, H., Ohno, H., Bonifacino, J.S., and Mellman, I. (1999). A novel clathrin adaptor complex mediates basolateral targeting in polarized epithelial cells. Cell *99*, 189–198.

Futter, C.E., Gibson, A., Allchin, E.H., Maxwell, S., Ruddock, L.J., Odorizzi, G., Domingo, D., Trowbridge, I.S., and Hopkins, C.R. (1998). In polarized MDCK cells basolateral vesicles arise from clathrin-gamma-adaptin-coated domains on endosomal tubules. J. Cell Biol. *141*, 611–623.

Galli, T., Chilcote, T., Mundigl, O., Binz, T., Niemann, H., and De Camilli, P. (1994). Tetanus toxin-mediated cleavage of cellubrevin impairs exocytosis of transferrin receptor-containing vesicles in CHO cells. J. Cell Biol. *125*, 1015–1024.

Geuze, H.J., Slot, J.W., and Schwartz, A.L. (1987). Membranes of sorting organelles display lateral heterogeneity in receptor distribution. J. Cell Biol. *104*, 1715–1723.

Gossen, M., and Bujard, H. (1992). Tight control of gene expression in mammalian cells by tetracycline-responsive promotors. Proc. Natl. Acad. Sci. USA *89*, 5547–5551.

Haylett, T., and Thilo, L. (1986). Limited and selective transfer of plasma membrane glycoproteins to membrane of secondary lysosomes. J. Cell Biol. *103*, 1249–1256.

Henley, J.R., and McNiven, M.A. (1996). Association of a dynamin-like protein with the Golgi apparatus in mammalian cells. J. Cell Biol. *133*, 761–775.

Herskovits, J.S., Burgess, C.C., Obar, R.A., and Vallee, R.B. (1993). Effects of mutant rat dynamin on endocytosis. J. Cell Biol. *122*, 565–578.

Hopkins, C.R., Gibson, A., Shipman, M., Strickland, D.K., and Trowbridge, I.S. (1994). In migrating fibroblasts, recycling receptors are concentrated in narrow tubules in the pericentriolar area, and then routed to the plasma membrane of the leading lamella. J. Cell Biol. *125*, 1265–1274.

Hopkins, C.R., and Trowbridge, I.S. (1983). Internalization and processing of transferrin and the transferrin receptor in human carcinoma A431 cells. J. Cell Biol. *97*, 508–521.

Johnson, L.S., Dunn, K.W., Pytowski, B., and McGraw, T.E. (1993). Endosome acidification and receptor trafficking: bafilomycin A1 slows receptor externalization by a mechanism involving the receptor's internalization motif. Mol. Biol. Cell *4*, 1251–1266.

Jones, S.M., Howell, K.E., Henley, J.R., Cao, H., and McNiven, M.A. (1998). Role of dynamin in the formation of transport vesicles from the trans-Golgi network. Science *279*, 573–577.

Kreis, T.E. (1987). Microtubules containing detyrosinated tubulin are less dynamic. EMBO J. *6*, 2597–2606.

Lin, S.X., Grant, B., Hirsh, D., and Maxfield, F.R. (2001). Rme-1 regulates the distribution and function of the endocytic recycling compartment in mammalian cells. Nat. Cell Biol. *3*, 567–572.

Maier, O., Knoblich, M., and Westermann, P. (1996). Dynamin II binds to the trans-Golgi network. Biochem. Biophys. Res. Commun. *223*, 229–233.

Marsh, M., and McMahon, H.T. (1999). Cell biology: the structural era of endocytosis. Science *285*, 215–220.

Mayor, S., Presley, J.F., and Maxfield, F.R. (1993). Sorting of membrane components from endosomes and subsequent recycling to the cell surface occurs by a bulk flow process. J. Cell Biol. *121*, 1257–1269.

Mellman, I. (1996). Endocytosis and molecular sorting. Annu. Rev. Cell Dev. Biol *12*, 575–625.

Mu, F.T., Callaghan, J.M., Steele-Mortimer, O., Stenmark, H., Parton, R.G., Campbell, P.L., McCluskey, J., Yeo, J.P., Tock, E.P., and Toh, B.H. (1995). EEA1, an early endosome-associated protein: EEA1 is a conserved alpha-helical peripheral membrane protein flanked by cysteine "fingers" and contains a calmodulin-binding IQ motif. J. Biol. Chem. *270*, 13503–13511.

Newmyer, S.L., and Schmid, S.L. (2001). Dominant-interfering Hsc70 mutants disrupt multiple Stages of the clathrin-coated vesicle cycle in vivo. J. Cell Biol. *152*, 607–620.

Nicoziani, P., Vilhardt, F., Llorente, A., Hilout, L., Courtoy, P.J., Sandvig, K., and van Deurs, B. (2000). Role for dynamin in late endosome dynamics and trafficking of the cation-independent mannose 6-phosphate receptor. Mol. Biol. Cell *11*, 481–495.

Odorizzi, G., and Trowbridge, I.S. (1997). Structural requirements for basolateral sorting of the human transferrin receptor in the biosynthetic and endocytic pathways of Madin-Darby canine kidney cells. J. Cell Biol. *137*, 1255–1264.

Omary, M.B., and Trowbridge, I.S. (1981). Biosynthesis of the human transferrin receptor in cultured cells. J. Biol. Chem. *256*, 12888–12892.

Prekeris, R., Klumperman, J., Chen, Y.A., and Scheller, R.H. (1998). Syntaxin 13 mediates cycling of plasma membrane proteins via tubulovesicular recycling endosomes. J. Cell Biol. *143*, 957–971.

Prescott, A.R., Lucocq, J.M., James, J., Lister, J.M., and Ponnambalam, S. (1997). Distinct compartmentalization of TGN46 and beta 1,4-galactosyltransferase in HeLa cells. Eur. J. Cell Biol. *72*, 238–246.

Presley, J.F., Mayor, S., Mcgraw, T.E., Dunn, K.W., and Maxfield, F.R. (1997). Bafilomycin A(1) treatment retards transferrin receptor recycling more than bulk membrane recycling. J. Biol. Chem. *272*, 13929–13936.

Ren, M.D., Xu, G.X., Zeng, J.B., Delemoschiarandini, C., Adesnik, M., and Sabatini, D.D. (1998). Hydrolysis of GTP on rab11 is required for the direct delivery of transferrin from the pericentriolar recycling compartment to the cell surface but not from sorting endosomes. Proc. Natl. Acad. Sci. USA *95*, 6187–6192.

Sever, S., Damke, H., and Schmid, S.L. (2000). Dynamin:GTP controls the formation of constricted coated pits, the rate limiting step in clathrin-mediated endocytosis. J. Cell Biol. *150*, 1137–1148.

Sheff, D.R., Daro, E.A., Hull, M., and Mellman, I. (1999). The receptor recycling pathway contains two distinct populations of early endosomes with different sorting functions. J. Cell Biol. *145*, 123–139.

Siddhanta, U., McIlroy, J., Shah, A., Zhang, Y., and Backer, J.M. (1998). Distinct roles for the p110alpha and hVPS34 phosphatidylinositol 3′-kinases in vesicular trafficking, regulation of the actin cytoskeleton, and mitogenesis. J. Cell Biol. *143*, 1647–1659.

Sönnichsen, B., De Renzis, S., Nielsen, E., Rietdorf, J., and Zerial, M. (2000). Distinct membrane domains on endosomes in the recycling pathway visualized by multicolor imaging of Rab4, Rab5, and Rab11. J. Cell Biol. *149*, 901–914.

Stoorvogel, W., Geuze, H.J., Griffith, J.M., and Strous, G.J. (1988). The pathways of endocytosed transferrin and secretory protein are connected in the trans-Golgi reticulum. J. Cell Biol. *106*, 1821–1829.

Stoorvogel, W., Geuze, H.J., and Strous, G.J. (1987). Sorting of endocytosed transferrin and asialoglycoprotein occurs immediately after internalization in HepG2 cells. J. Cell Biol. *104*, 1261–1268.

Stoorvogel, W., Oorschot, V., and Geuze, H.J. (1996). A novel class of clathrin-coated vesicles budding from endosomes. J. Cell Biol. *132*, 21–33.

Teter, K., Chandy, G., Quinones, B., Pereyra, K., Machen, T., and Moore, H.P.H. (1998). Cellubrevin-targeted fluorescence uncovers heterogeneity in the recycling endosomes. J. Biol. Chem. *273*, 19625–19633.

Ullrich, O., Reinsch, S., Urbe, S., Zerial, M., and Parton, R.G. (1996). Rab11 regulates recycling through the pericentriolar recycling endosome. J. Cell Biol. *135*, 913–924.

Urrutia, R., Henley, J.R., Cook, T., and McNiven, M.A. (1997). The dynamins: redundant or distinct functions for an expanding family of related GTPases? Proc. Natl. Acad. Sci. USA *94*, 377–384.

van der Bliek, A.M. (1999). Functional diversity in the dynamin family. Trends Cell Biol. *9*, 96–102.

van der Bliek, A.M., Redelmeier, T.E., Damke, H., Tisdale, E.J., Meyerowitz, E.M., and Schmid, S.L. (1993). Mutations in human dynamin block an intermediate stage in coated vesicle formation. J. Cell Biol. *122*, 553–563.

van der Sluijs, P., Hull, M., Webster, P., Male, P., Goud, B., and Mellman, I. (1992). The small GTP-binding protein rab4 controls an early sorting event on the endocytic pathway. Cell *70*, 729–740.

van Weert, A.W., Dunn, K.W., Geuze, H.J., Maxfield, F.R., and Stoorvogel, W. (1995). Transport from late endosomes to lysosomes, but not sorting of integral membrane proteins in endosomes, depends on the vacuolar proton pump. J. Cell Biol. *130*, 821–834.

Ward, D.M., Perou, C.M., Lloyd, M., and Kaplan, J. (1995). "Synchronized" endocytosis and intracellular sorting in alveolar macrophages: the early sorting endosome is a transient organelle. J. Cell Biol. *129*, 1229–1240.

White, S., Miller, K., Hopkins, C., and Trowbridge, I.S. (1992). Monoclonal antibodies against defined epitopes of the human transferrin receptor cytoplasmic tail. Biochim. Biophys. Acta *1136*, 28–34.

Wilcke, M., Johannes, L., Galli, T., Mayau, V., Goud, B., and Salamero, J. (2000). Rab11 regulates the compartmentalization of early endosomes required for efficient transport from early endosomes to the trans-Golgi network. J. Cell Biol. *151*, 1207–1220.

Yamashiro, D.J., Tycko, B., Fluss, S.R., and Maxfield, F.R. (1984). Segregation of transferrin to a mildly acidic (pH 6.5) para-Golgi compartment in the recycling pathway. Cell *37*, 789–800.